

Supporting Information

High-pressure-triggered homodisperse for the reconstruction of graphene nanosheets towards Na ion storage

In this study, a series of graphene samples with varying interlayer spacings were prepared using a simple microfluidization method [1,2]. High-pressure homogenization was employed to reconstruct the graphene nanosheets for efficient Na ion storage. This approach involves controlling the amount of intercalated graphite (GNPs) in an aqueous dispersion of graphene oxide (GO) to adjust the interlayer spacing. The electrostatic behavior was observed based on the surface charge of GO and GNPs [18]. [3]. Through microfluidization methods, the heterogeneous interface of GNPs-GO layer material was formed via self-assembly of GNPs and GO. The potential reaction process is illustrated in Figure 1a. Considering the physical dimensions of the high-pressure homogenizer system, approximately ~1270J energy was generated by applying 50MPa for 5 cycles, surpassing the exfoliation energy (~455 J) required for 1g graphite. Among them, graphene oxide (GO) plays a crucial role as a surfactant due to its hydrophilic oxidation functional groups and hydrophobic carbon skeleton, which enables it to effectively balance the charge with gold nanoparticles (GNPs). The self-assembled process results in the formation of various heterogeneous interfaces depending on the ratio of GO to GNPs. This is illustrated in Figure S1, which demonstrates different dispersion behaviors upon addition of varying ratios of GNPs and GO suspension.

The increased GNPs disrupt the balance of electrostatic attraction and repulsion, resulting in a charge mismatch that leads to severe agglomeration. The dispersion stability of GO-GNPs is significantly influenced by the ratio of GNPs, as it can be observed that a solution with excellent dispersion cannot be formed beyond 60wt% due to the limited presence of defect-free and functional group-rich GNPs, which are difficult to disperse without sufficient GO. The good dispersion is crucial for achieving a stable GNPs-GO heterogeneous interface, as it greatly influences the interlayer spacing of the GNPs-GO layer material. In order to investigate the stability behavior of the heterogeneous interface, vacuum filtration was conducted on 15wt%, 30wt%, 45wt%, 60wt%, 75% and 90wt% GNPs-GO suspensions. The resulting image, shown in Figure S3, confirmed that poor dispersion prevents the formation of a freestanding film.

Note 1

A theoretical probe approach curve (PAC) can be calculated according to the following equation based on the numerical method:

$$i_{T,\infty} = 4nFDc_0r_t$$

$$I_T = \frac{i_T}{i_{T,\infty}}$$

$$I_T^K = I_S^K \left(1 - \frac{I_T^{ins}}{I_T^{con}} \right)$$

$$I_S^K = \frac{0.78377}{L \left(1 + \frac{1}{\Lambda} \right)} + \frac{0.68 + 0.3315 \exp(-1.0672/L)}{1 + F(L,\Lambda)}$$

$$\Lambda = k_{eff}a/D_0$$

$$F(L,\Lambda) = \frac{(11 + 7.3\Lambda)}{(\Lambda(110 - 40L))}$$

$$I_T^{ins}(L, RG) = \frac{(2.08/RG^{0.358})(L - (0.145/RG)) + 1.585}{(2.08/RG^{0.358})(L + 0.00238RG) + 1.57 + (\ln RG/L) + (2/\pi RG) \ln(1 + (\pi RG/2L))}$$

$$I_T^{con}(L + \kappa^{-1}, RG) = \alpha(RG) + \frac{\pi}{4\beta(RG) \arctan\left(\frac{1}{L + \kappa^{-1}}\right)} + \left(1 - \alpha(RG) - \frac{1}{2\beta(RG)} \right) \frac{2}{\pi} \arctan\left(\frac{1}{L + \kappa^{-1}}\right)$$

$$\alpha(RG) = \ln 2 + \ln 2 \left(1 - \frac{2}{\pi} \arccos\left(\frac{1}{RG}\right) \right) - \ln 2 \left(1 - \left(\frac{2}{\pi} \arccos\left(\frac{1}{RG}\right) \right)^2 \right)$$

$$\beta(RG) = 1 + 0.639 \left(1 - \frac{2}{\pi} \arccos\left(\frac{1}{RG}\right) \right) - 0.186 \left(1 - \left(\frac{2}{\pi} \arccos\left(\frac{1}{RG}\right) \right)^2 \right)$$

Where $i_{T,\infty}$ is steady-state current, n is number of electrons transferred, F is Faraday constant, D is diffusion coefficient, c_0 is initial concentration of solution, r_t is radius of UME, I_T is the normalized tip current, k_{eff} is the first-order heterogeneous rate constant, κ is the heterogeneous rate constant, RG is the ratio between the radius of the glass capillary tube and the radius of the molybdenum disk in the ultramicroelectrode, I_T^{con} , I_T^K and I_T^{ins} represent the normalized tip currents for diffusion-controlled regeneration of a redox mediator, finite substrate kinetics, and insulating substrate (i.e., no mediator regeneration), respectively.

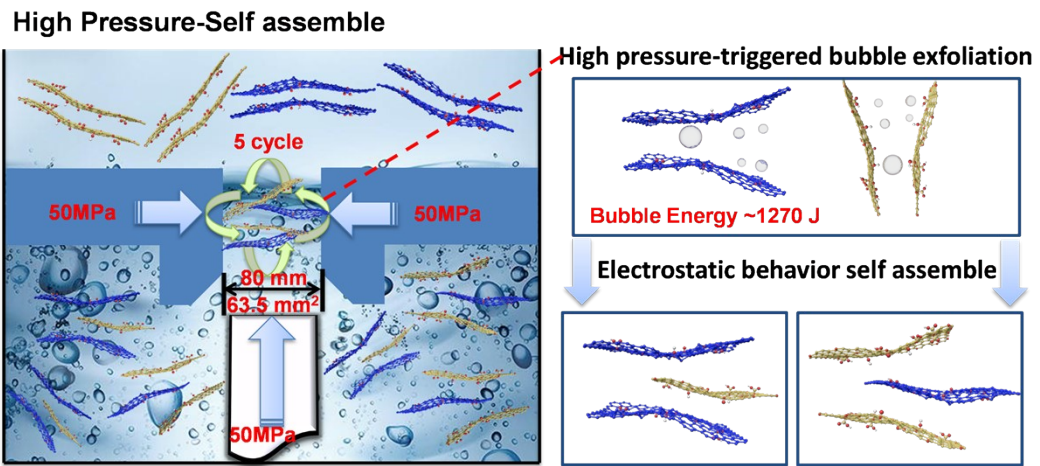


Figure S1 The possible reconstruction process of the heterogeneous interface with different ratio of GNPs and GO.

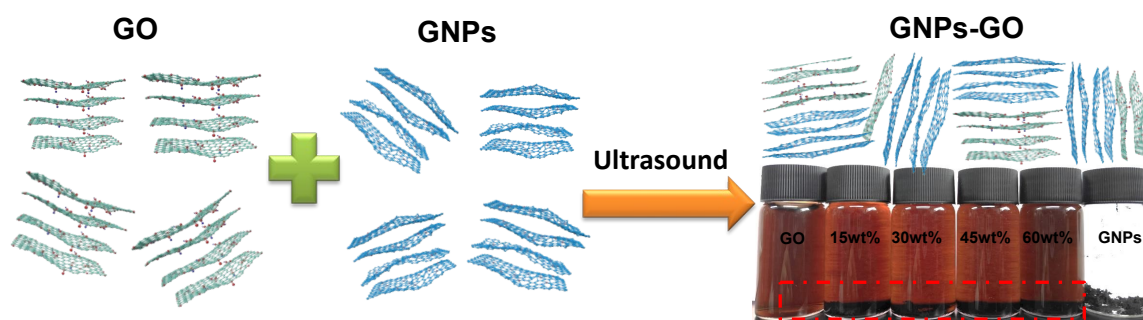


Figure S2 The the ultrasonic dispersion process and the digital photos of different ratio of GNPs and GO dispersion.

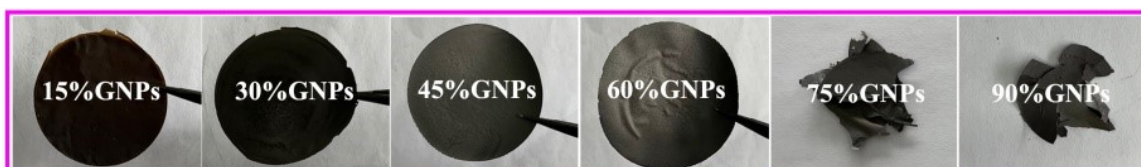


Figure S3 The digital photos of films via vacuum filtration with different GO and GNPs content:From left to right: 15wt%, 30wt%, 45wt% and 60wt% GNPs-GO and GNPs.

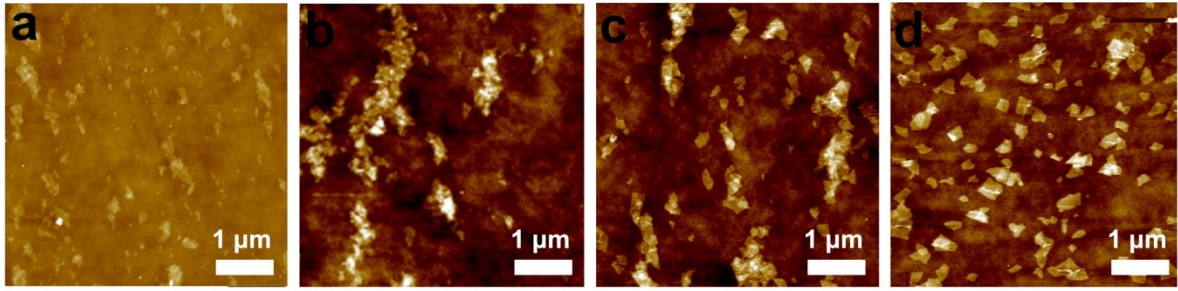


Figure S4 The AFM images of (a) 15wt%GNPs-GO, (b) 30wt%GNPs-GO, (c) 45wt%GNPs-GO, (d) 60wt%GNPs-GO.

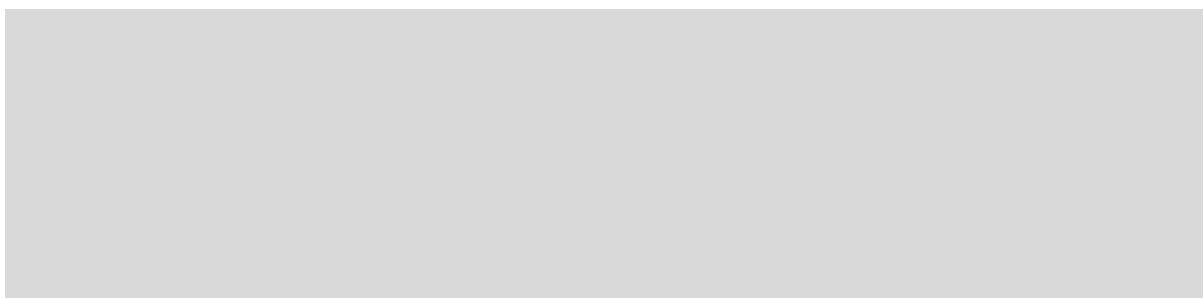


Figure S5 The AFM images of (a) and (b) 75wt%GNPs-GO.

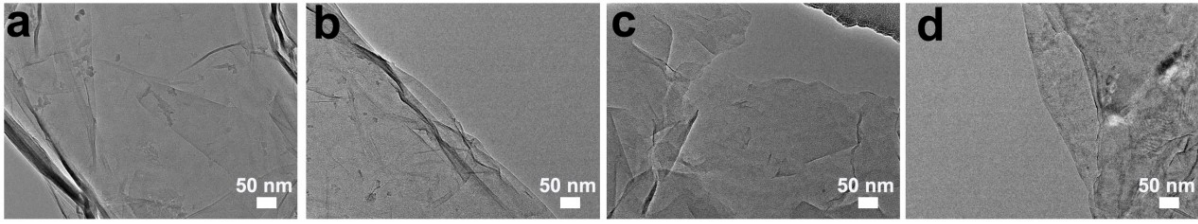


Figure S6 The TEM images of (a) 15wt%, (b)30wt%, (c)45wt% and (d) 60wt% GNPs-GO.

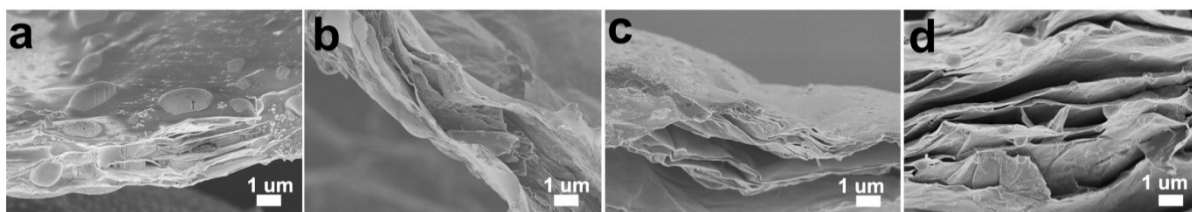


Figure S7 The SEM images of cross-section of (a)15wt%GNPs-RGO, (b)30wt%GNPs-RGO, (c)45wt%GNPs-RGO,(d) and 60wt%GNPs-RGO

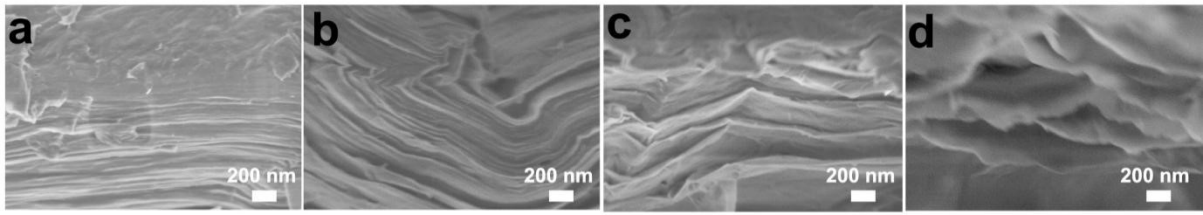


Figure S8 The SEM images of cross-section of (a) 15wt%, (b)30wt%, (c)45wt% and (d) 60wt% GNPs-GO.

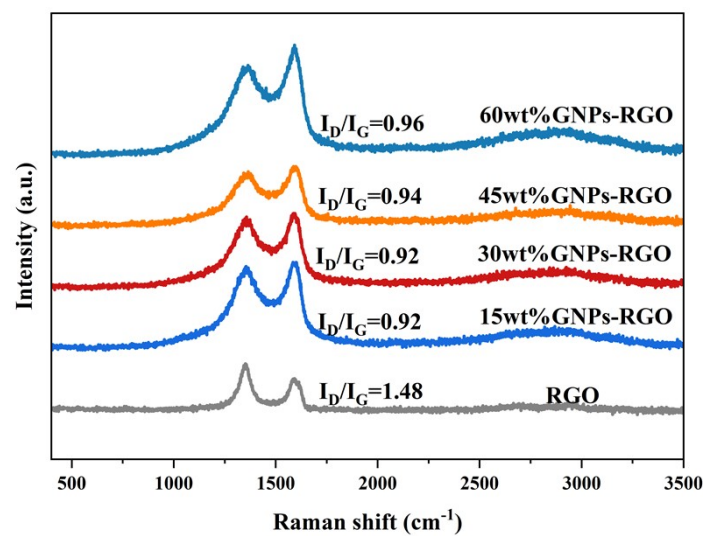


Figure S9 Raman spectra of GNPs-GO after reduction

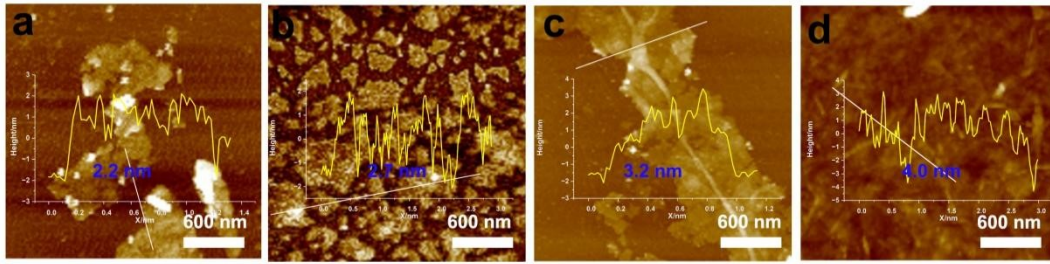


Figure S10 The AFM images and their thickness-distributions of (a) 15 wt% GNPs-RGO, (b) 30 wt% GNPs-RGO, (c) 45 wt% GNPs-RGO, and (d) 60 wt% GNPs-RGO.

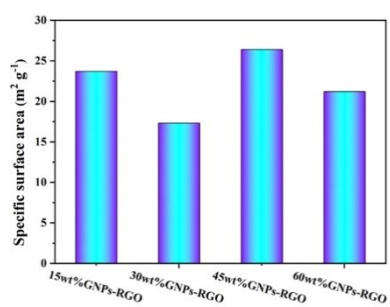


Figure S11 The specific surface areas of 15wt%, 30wt%, 45wt% and 60wt% GNPs-RGO.

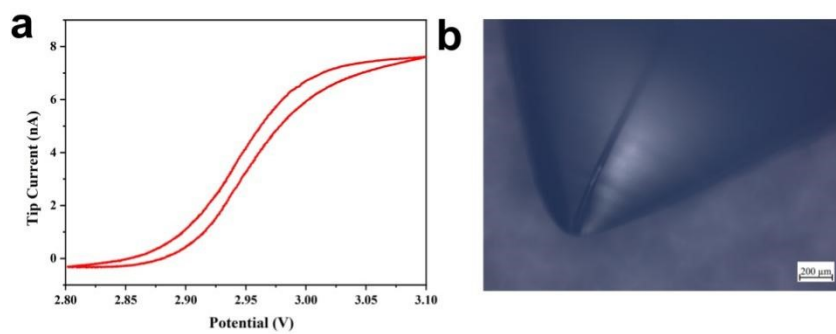


Figure S12 (a) A reversible CV curve of the SECM system. (b) Optical micrograph of 12.5 μm radius Pt UME.

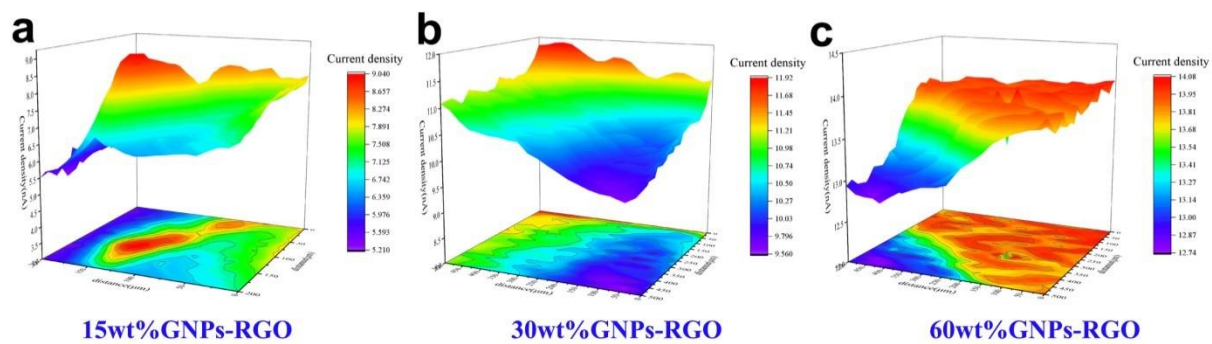


Figure S13 SECM current density performance of (a) 15 wt% GNPs-RGO; (b) 30 wt% GNPs-RGO; (c) 60 wt% GNPs-RGO.

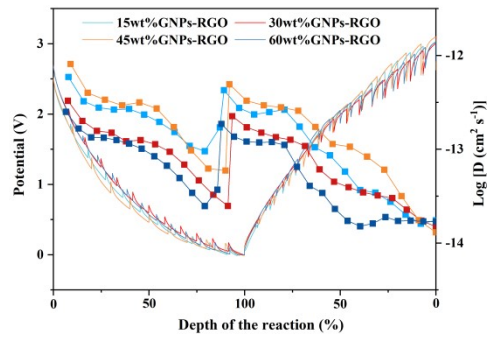


Figure S14 GITT curves of GNPs-RGO

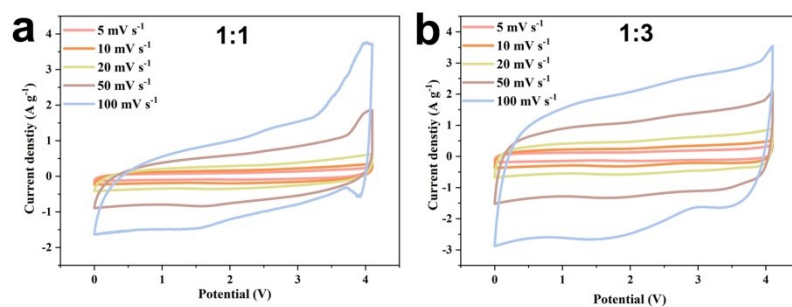


Figure S15 CVs of 45 wt% GNPs-RGO//AC with different mass ratios: (a) 1:1, (b) 1:3

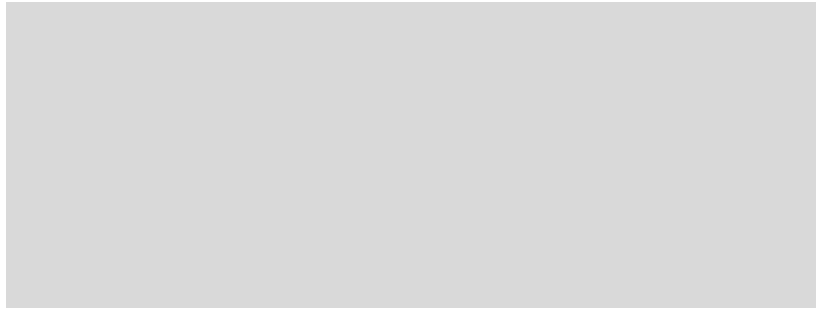


Figure S16 GCD profiles of 45 wt% GNPs-RGO//AC with different mass ratios: (a) 1:1, (b) 1:3

Table S1 the detailed content of all functional groups.

Sample name	C-C	C=C	C-O
15wt%GNPs-RGO	59.39	24.11	16.50
30wt%GNPs-RGO	62.45	21.93	15.61
45wt%GNPs-RGO	69.51	19.84	10.65
60wt%GNPs-RGO	73.53	16.03	10.44

Notes and references

1. Yang J, Zhang X, Liu Y, Tai Z, Yan X, Ma J. *Adv Materials Inter*, 2021, 8: 2001899
2. Shen Z, Li J, Yi M, Zhang X, Ma S. *Nanotechnology*, 2011, 22: 365306
3. Li Z, Gadipelli S, Li H, Howard CA, Brett DJL, Shearing PR, Guo Z, Parkin IP, Li F. *Nat Energy*, 2020, 5: 160–168